

1 **The Occlusion Effects in Capacitive Contact Imaging for *In-vivo* Skin Damage**

2 **Assessments**

3

4 Wei Pan¹, Xu Zhang¹, Majella Lane² and Perry Xiao¹ *

5

6 ¹School of Engineering, London South Bank University, 103 Borough Road, London

7 SE1 0AA, United Kingdom

8 ²UCL School of Pharmacy, 29-39 Brunswick Square, London WC1N 1AX, United

9 Kingdom

10

11 * Corresponding Author, Tel: 00 44 20 7815 7569 Fax: 00 44 20 7815 7561

12 email: xiaop@lsbu.ac.uk

13

1 **The Occlusion Effects in Capacitive Contact Imaging for *In-vivo* Skin Damage**

2 **Assessments**

3

4 **Abstract**

5 **OBJECTIVE:** The aim of this study is to investigate the occlusion effects in
6 capacitive contact imaging, in order to develop a new quantitative methodology for
7 *in-vivo* skin assessments by using capacitive contact imaging and
8 condenser-TEWL(trans-epidermal water loss) method.

9

10 **METHODS:** Two measurement technologies were used in this study, i.e. capacitive
11 contact imaging and condenser-TEWL method. Three types of skin damages were
12 studied, e.g. intensive washes, tape stripping, and sodium lauryl sulfate (SLS)
13 irritation. The test skin sites were chosen on the volar forearms of healthy
14 volunteers (aged 25 - 45), the measurements were performed both before and
15 periodically after the damages.

16

17 **RESULTS:** The results show that the time-dependent occlusion curves of
18 capacitive contact imaging can reflect the types of damages, and by analyzing the
19 shapes of the curves we can get information about the skin surface water content

20 level and stratum corneum thickness. The results also show that the combination of
21 capacitive contact imaging and condenser-TEWL method gives extra information
22 about the skin damages, such as the types of the damages and status of the
23 damages.

24

25 **CONCLUSION:** We have developed a potential new quantitative methodology for
26 skin damage assessments by using capacitive contact imaging and
27 condenser-TEWL method. The combination of the two technologies can provide
28 useful information for skin damage assessments. We have also developed a
29 mathematical model for analyzing the occlusion curves.

30

31 **Keywords**

32 Skin occlusion, capacitive contact imaging, skin damage assessments, skin
33 hydration, TEWL.

34

35 **1. Introduction**

36 Skin damage is a very important issue for occupational health as well as
37 environmental threat [1,2]. However, to assess the skin damage is not easy,
38 especially quantitatively. To date, skin damage assessments are largely done

39 through visual assessments, which can be subjective and difficult to quantify. There
40 is a need to develop a new, quantitative, and simple methodology that can quantify
41 the skin damage assessments. We know that water in stratum corneum (SC) plays
42 an important role in skin's cosmetic properties as well as its barrier functions, and
43 SC water concentration and trans-epidermal water loss (TEWL) are two key
44 indexes for skin characterizations [3,4]. In this paper, we present our latest study on
45 the occlusion effects in capacitive contact imaging for *in-vivo* skin damage
46 assessments. Capacitive contact imaging based fingerprint sensors, originally
47 designed for biometric applications, has shown potential for skin hydration imaging,
48 surface analysis, 3D surface profile, skin micro-relief as well as solvent penetration
49 measurements [5-11]. With the capacitive contact imaging, we can measure the
50 skin surface water concentration distribution map. By occluding the skin with
51 capacitive imaging sensor over a period of time, as water dynamically builds up
52 underneath the sensor surface due to the blockage of trans-epidermal water loss,
53 we can also generate time-dependent skin occlusive hydration curves. It is this
54 time-dependent occlusive hydration curves that we are mainly interested in this
55 study. Our previous studies have also shown that skin occlusion measurements can
56 differentiate normal skin and damaged skin [12]. The purpose of this study is to
57 develop a new methodology for skin damage assessments, which can even

58 differentiate different types of damages, by using skin capacitive contact imaging
59 occlusion measurements, as well as the trans-epidermal water loss (TEWL)
60 measurements.

61

62 **2. Materials and Methods**

63 2.1 Instruments

64 The capacitive contact imaging technology developed by the research group [8-11]
65 is based on Fujistu fingerprint sensor (Fujistu Ltd, Japan), which has a matrix of 256
66 × 300 pixels, with 50 µm spatial resolution per pixel. The fingerprint sensor basically
67 generates capacitance images of the skin surface. In each image, each pixel is
68 represented by an 8 bit grayscale value, 0~255, higher grayscale values mean
69 higher water concentration, and lower grayscale values mean lower water
70 concentration.

71

72 The TEWL measurements were performed by using the condenser-TEWL method
73 (AquaFlux, Biox Systems Ltd, UK), which is a condenser based closed-chamber
74 measurement technology [13,14]. Its cylindrical measurement chamber is open at
75 the end placed onto the skin surface, and closed by means of a condenser cooled
76 below the freezing temperature of water at the other end. This design provides a

77 controlled measurement environment, which enhances the repeatability and
78 accuracy of the measurements.

79

80 2.2 Mathematical Modeling of Skin Occlusion

81 According to diffusion theory, the skin occlusion can be described by following one
82 dimensional diffusion equation with following initial condition and boundary
83 condition.

84

$$85 \quad \begin{cases} D(H) \frac{\partial^2 H}{\partial z^2} = \frac{\partial H}{\partial t}, & 0 \leq z \leq L \\ H(z, 0) = f(z) \\ H(L, t) = H_1 \\ -D \frac{\partial H}{\partial z} \Big|_{z=0} = 0 \end{cases} \quad (1)$$

86

87 where $H(z,t)$ is the skin water content at depth z and time t , L is SC thickness, $D(H)$
88 is the SC water diffusion coefficient, which is a function of water content $H(z,t)$, $f(z)$
89 is the initial skin water distribution within SC. In this case, we can assume it is a
90 linear distribution, defined by

$$91 \quad f(z) = H_0 + \frac{H_1 - H_0}{L} \times z. \quad (2)$$

92 where H_0 is the SC surface water concentration, and H_1 is the SC bottom water
93 concentration. In Eq.(1), at the skin surface ($z=0$), there is zero flux due to occlusion,
94 and at the SC bottom ($z=L$), we assume there is a constant water concentration H_1 .

95 We can solve the Eq.(1) by substituting Eq.(2) into Eq.(1), and the solution can be

96 expressed as,

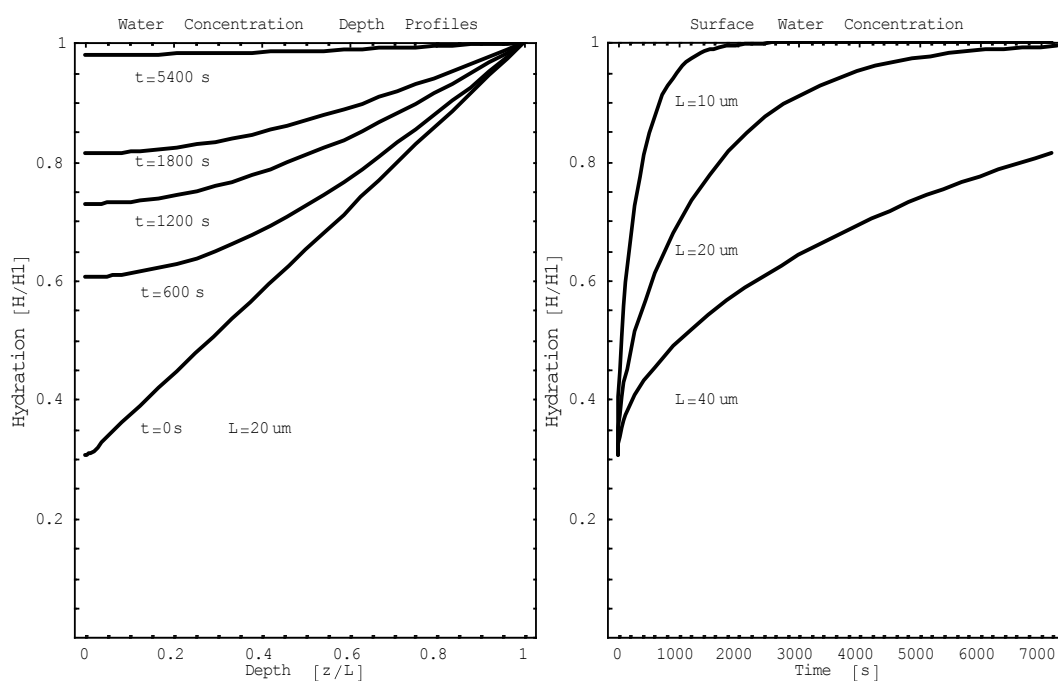
97

$$98 \quad H(z, t) = H_1 + \frac{2}{L} \sum_{n=0}^{\infty} \left(e^{-\frac{D(2n+1)^2 \pi^2 t}{4L^2}} \times \cos \frac{(2n+1)\pi z}{2L} \times \left(\frac{2L(-1)^{n+1} H_1}{(2n+1)\pi} + \right. \right.$$

$$99 \quad \left. \left. \frac{2L(H_1(2n+1)\pi \cos(n\pi) + 2(H_1 - H_0)(1 + \sin(n\pi)))}{(2n+1)^2 \pi^2} \right) \right)$$

100 (3)

101



102

103 Figure 1 The SC normalized water concentration depth profiles at different time

104 during the occlusion with $L=20\mu\text{m}$ (left), and the time dependent normalized surface

105 water concentration levels of three different SC thickness (right).

106

107 Figure 1 shows results of above solution, the left plot shows the SC water
108 concentration depth profiles at different time during the occlusion, using normalized
109 the depth (z/L , $L=20\mu\text{m}$) and normalized water concentration (H/H_1 , $H_1=80\%$
110 $H_0=24\%$), and right plot shows the time dependent normalized surface water
111 concentration (H/H_1 , $H_1=80\%$ $H_0=24\%$) levels of three different SC thickness
112 ($L=10\mu\text{m}$, $20\mu\text{m}$, $40\mu\text{m}$).

113

114 The results show that different SC thicknesses have different times to reach steady
115 state, for a SC with $20\mu\text{m}$ thickness, which is typical SC thickness in volar forearm,
116 it is about 30 minutes to reach 80% of H_1 and about 2 hours to reach the steady
117 state, i.e. 100% of H_1 .

118

119 2.3 Experimental Procedures

120 In this paper, skin sites on volar forearms of **three** healthy volunteers, aged 25 - 45,
121 were chosen for the measurements. The skin test sites were deliberately damaged
122 by intensive washes, tape stripping **or** sodium lauryl sulfate (SLS) irritation. **Three**
123 **measurements were performed at different period of time, and only one test site**
124 **was chosen on each forearm, to avoid cross interference. The measurements were**
125 **repeated a few times, to make sure the results are repeatable, but only one set of**

126 the data was presented. Intensive washing used room temperature running water
127 and washing-up liquid, rubbing the site gently for 3 minutes with a finger. After each
128 wash, the skin site was carefully patted dry with a tissue before the measurements.
129 Tape stripping was performed 20 times per site by the use of standard stripping
130 tape. SLS irritation was achieved by applying 2% SLS water solution (v/v, volume
131 ratio) on skin. Capacitive contact imaging measurements and TEWL measurements
132 were performed both before and immediately after the skin was damaged. They
133 were both on the same skin site, with capacitive contact imaging measurements
134 performed after the TEWL measurements, which took about 1 minute. The skin
135 occlusion measurements using capacitive contact imaging to occlude the skin test
136 sites for a period of one minute, during which skin capacitance images were
137 recorded continuously. The average grayscale values of the images were then
138 calculated at different times during occlusion. Since grayscale values are
139 proportional to SC hydration [8,11], the plots of grayscale value against time, can be
140 interpreted as SC hydration against time.

141

142 All the measurements were performed under normal ambient laboratory conditions,
143 of 20-21°C, and 40-50% RH. The volar forearm skin sites used were initially wiped

144 clean with ETOH/H₂O (95/5) solution. The volunteers were then acclimatized in the
145 laboratory for 20 minutes prior to the experiments.

146

147 **3 Results and Discussions**

148 3.1 The Occlusion Curves

149 Figure 2 shows capacitive contact imaging occlusion curves and corresponding
150 TEWL results of intensive washes, tape stripping and SLS irritation measurements.

151 The intensive washes produced small changes in the shapes of the contact imaging
152 occlusion curves. The general higher grayscale values of the occlusion curve
153 immediately after the washes indicate general higher SC hydration levels, which
154 may be caused by two factors, namely (i) superficial absorption of the water used in
155 the washes, and (ii) the removal of superficial SC cells during washing. After 25
156 minutes recovery time, the average grayscale values were found to have returned
157 to near-normal level. However, there is an undershoot, which suggests a
158 dehydration after the intensive washes, possibly due to the removal of some
159 superficial SC cells and the resultant loss of some SC barrier function. The TEWL
160 results follow a similar trend, and also confirmed the undershoot.

161

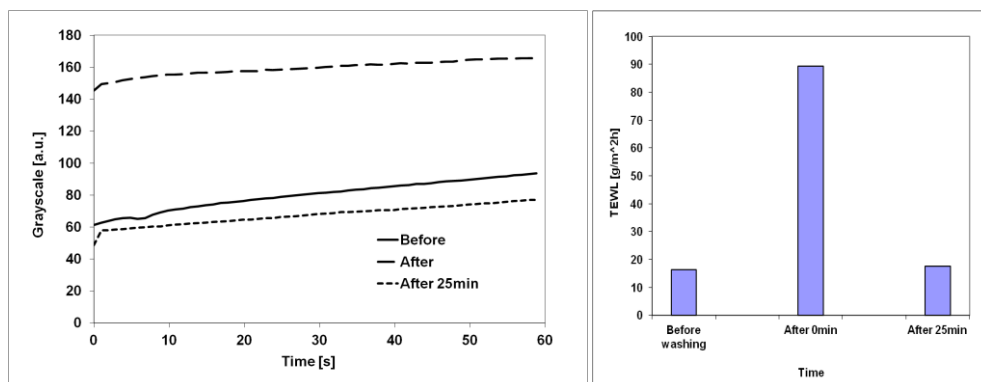
162 In tape stripping, the time dependent contact imaging occlusion curves show a
163 significant difference in shape (i.e. more curvature) between normal skin and
164 damaged skin. This curvature change reflects the SC structure change due to tape
165 stripping. Even after 60 minutes, the contact imaging occlusion curves were found
166 to be still significantly different from those of normal skin, indicating that SC was still
167 damaged. The TEWL values, however, has started returning to its normal value
168 after 60 minutes, indicating that although SC is still damaged, it starts to recover.

169

170 This curvature change can be confirmed by more detailed, longer time scale tape
171 stripping measurements, as shown in Figure 4. As the number of tape strips
172 increased, not only the level of contact imaging occlusion curves changed, but also
173 the curvature as well, with after 20 tape strips most significant, as shown in Figure 4
174 (left). Then as the skin recovery in the following days, the curvature of the contact
175 imaging occlusion curves gradually recovered to its normal level, as shown in
176 Figure 4 (right).

177

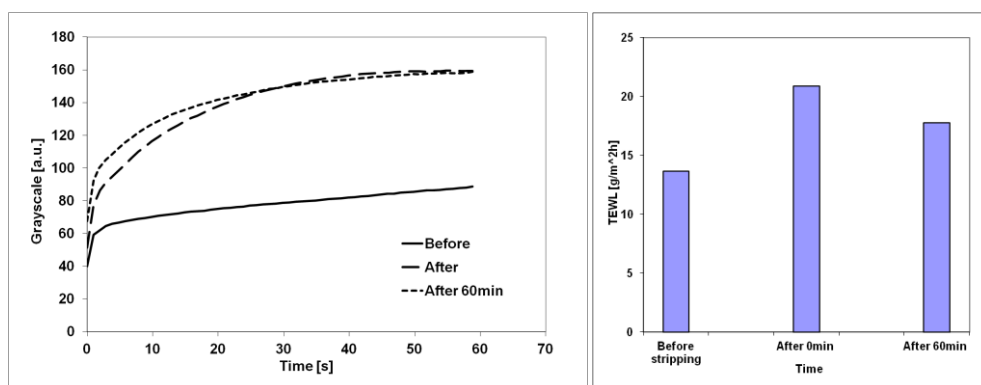
178



179

(a)

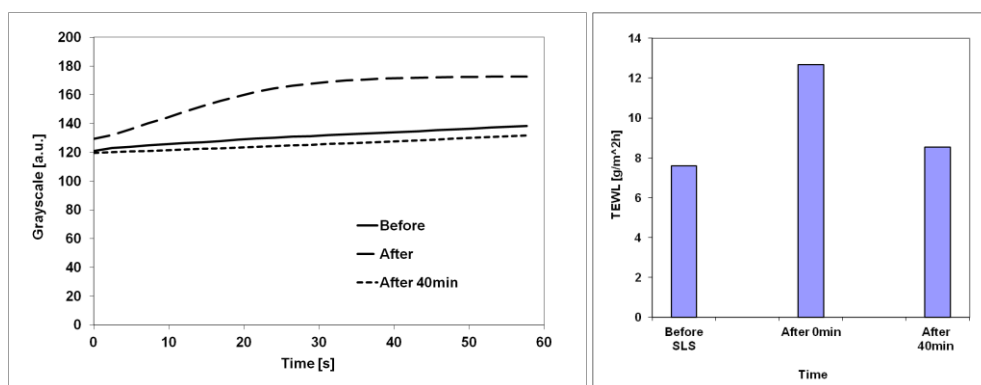
180



181

(b)

182



183

(c)

184 Figure 2. Skin capacitive contact imaging occlusion curves and corresponding

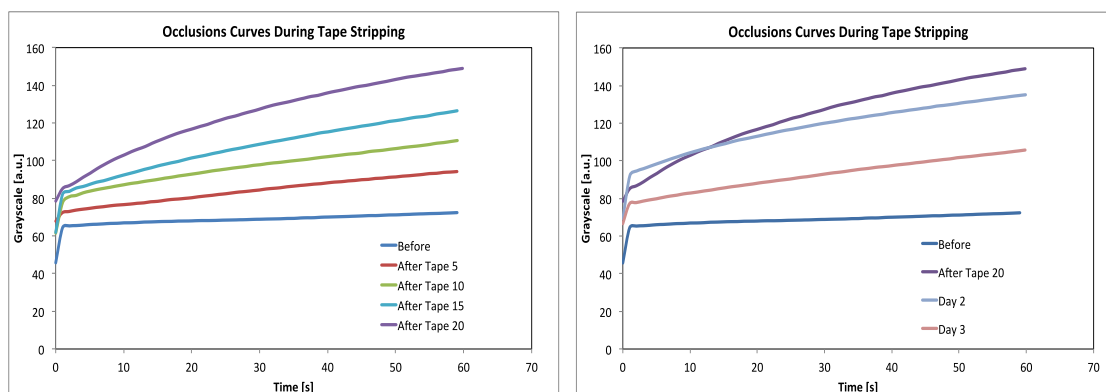
185 TEWL results of intensive washing (a); tape stripping (b); and SLS irritation (c).

186 Capacitive contact imaging measurements were taken after the TEWL

187 measurements, which were taken immediately after the damage, and each TEWL

188 measurement lasts about 1 minute.

189



190

191 Figure 3. Skin capacitive contact imaging occlusion curves during tape stripping

192 (left) and days after tape stripping (right).

193

194 Back to Figure 2, in SLS irritation, both the contact imaging occlusion curve and

195 TEWL value changed after irritation, but largely recovered after 40 minutes. It is

196 interesting to point out that the three types of skin damages produce three

197 distinctive occlusion curves, which indicates that, according to our theoretical

198 modeling, the SC surface hydration and SC structure are quite different under the

199 different types of skin damages. This suggests that the shapes of capacitive contact

200 imaging occlusion curves can provide extra information about skin damages. The

201 different types of damages changed skin surface hydration and structure differently

202 and therefore generated different types of occlusion curves. The results also show

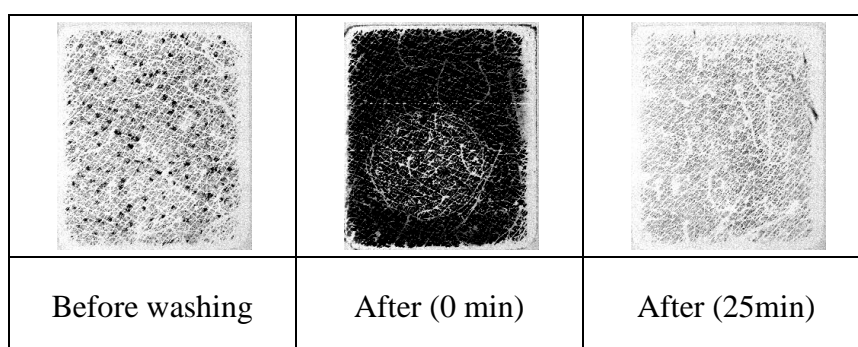
203 that TEWL results can reflect the skin damages, but can not differentiate the
204 damages. Therefore, the combination of capacitive contact imaging occlusion
205 measurements and TEWL measurements can provide more detailed,
206 comprehension information about skin damages.

207

208 Figure 4 shows corresponding capacitive contact images of intensive washes, tape
209 stripping and SLS irritation measurements. The skin images are generally getting
210 darker after damage, which indicates higher water content in SC. In both intensive
211 washes and SLS irritation, the lighter recovery skin images indicate there is a drying
212 effect after the damage. The lighter areas in the images immediately after the
213 intensive washing are imprints from the TEWL measurement head.

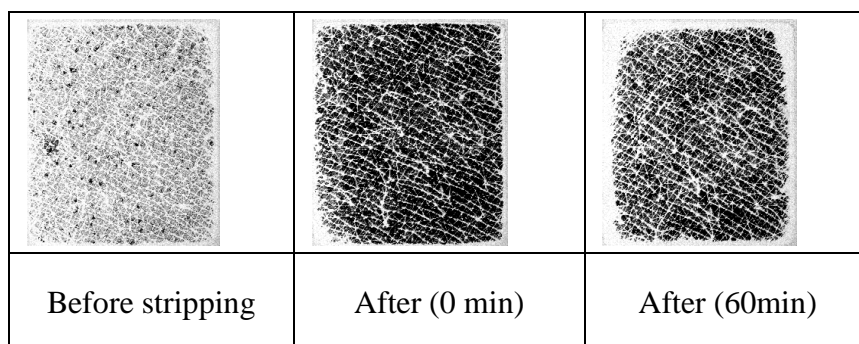
214

215



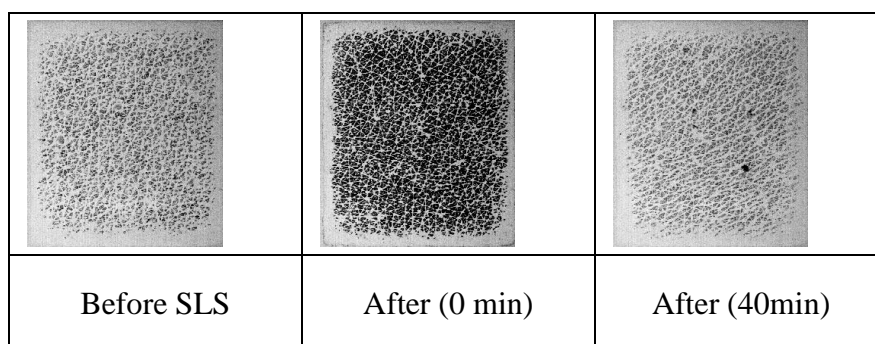
216

(a)



217

(b)



218

(c)

219 **Figure 4** Skin capacitive contact images of intensive washing (a); tape stripping (b);
 220 and SLS irritation (c).

221

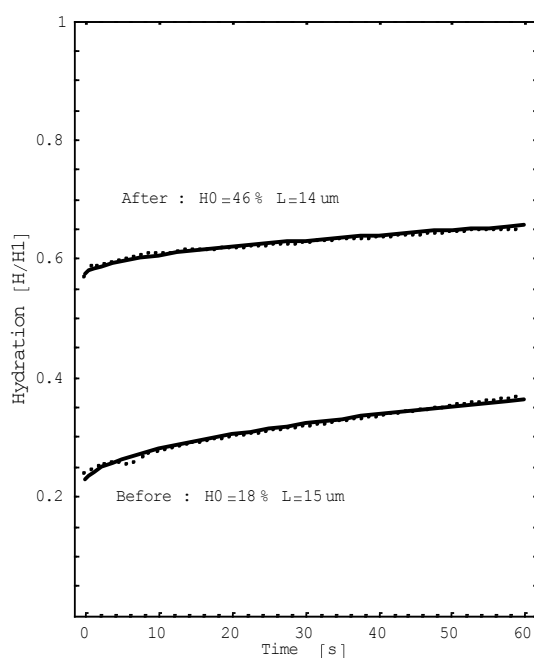
222 3.2 Comparison of Theoretical and Experimental Results

223 If we assume the maximum grayscale representing 100% water content, and zero
 224 grayscale represent 0% water content, then we can compare the theoretical results
 225 using Eq.(3) with above experimental results, see **Figure 5**. The comparison results
 226 show that the intensive washing has significantly increased the SC surface water
 227 content, but only slightly reduced the SC thickness, whilst the 20 tape stripping only
 228 slightly increase the SC surface water content, but significantly reduced the SC
 229 thickness. It is worth mentioning that the reduced SC thickness in theoretical

230 modeling data after SLS irritation is more likely to reflect the changes of water
231 distribution in SC, rather than the changes of SC structure. **The more pronounced**
232 **occlusion effect in Figure 5b is likely due to the significant skin structure changes**
233 **due to tape stripping.** Overall, the theoretical data matches better with normal skin
234 data, the significant mismatch of theoretical data and the data after 20 tape
235 stripping, indicate that tape stripping has significantly changed the structure of the
236 SC. Clearly, whence the capacitive contact imaging is calibrated, we will be able to
237 get the SC surface content and SC thickness values by **analyzing** the experimental
238 results using mathematical model described in Eq.(3).

239

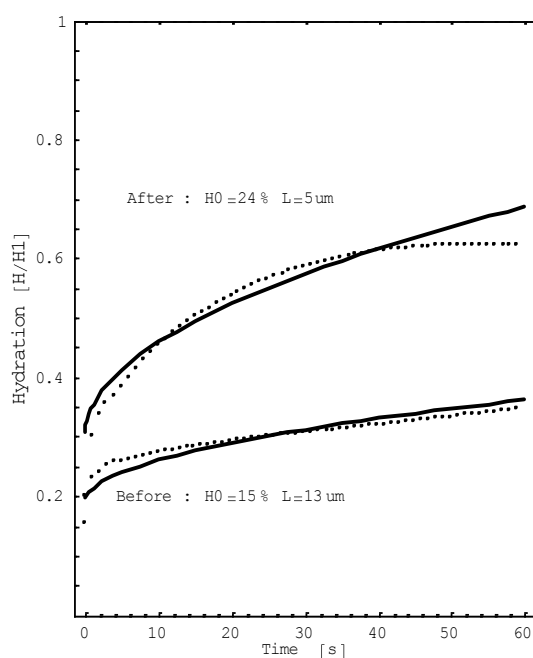
240



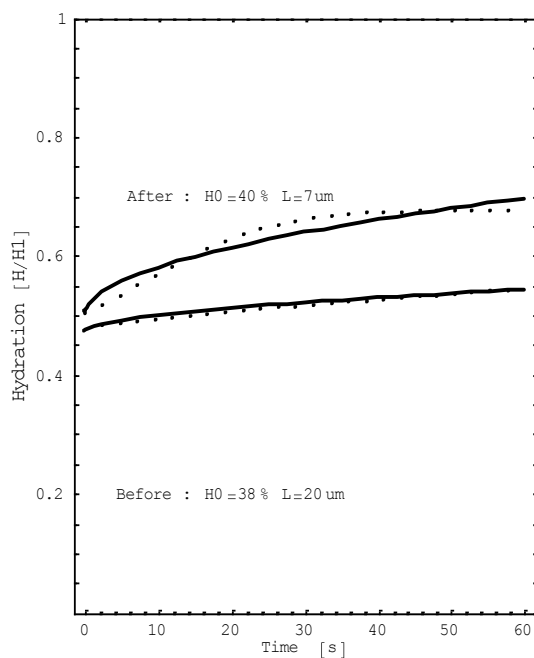
241

242

(a)



(b)



243

244

(c)

245 **Figure 5** The comparison of theoretical results and experimental results, the
246 intensive washing (a), the tape stripping (b), and SLS irritation (c).

247

248

249 **4 Conclusions and Future Works**

250 We have studied the occlusion effect in capacitive contact imaging for skin damage
251 assessments. The results show that the shapes of the capacitive contacting
252 imaging occlusion curves can be related to skin conditions, and different types of
253 skin damages have different shapes of occlusion curves. The TEWL measurements
254 can reflect the skin damages but can not differentiate different types of damages.
255 Therefore, the combination of skin occlusions using capacitive contact imaging and

256 TEWL measurements can provide useful, complementary information about skin
257 damage, and have potential as a new methodology for *in-vivo* skin damage
258 assessments. We have also developed a mathematical model for the skin occlusion,
259 the comparison of theoretical data and experimental data shows that the intensive
260 washes changes more of the SC surface water content, and the tape stripping
261 changes more of the SC thickness. The future work will be comparing the capacitive
262 contact imaging and TEWL measurements with other skin assessment
263 technologies, and to calibrate the capacitive contact imaging results, in order to
264 quantify the skin damage.

265

266 **References**

- 267 1. Dunitz M., The Environmental Threat to the Skin, Mark R and Plewig G (Ed.), The
268 University Press, Cambridge, ISBN 1-85317-057-7, 1992.
- 269 2. Grandjean P., Skin Penetration – Hazardous Chemicals at Work, Taylor &
270 Francis, London, ISBN 0-85066-834-4, 1990.
- 271 3. Fluhr J., Elsner P., Berardesca E., Maibach H.I. (Ed), Bioengineering of the Skin,
272 CRC Press, ISBN 0-8493-8374-9, 1995.
- 273 4. Fluhr J., Elsner P., Berardesca E., Maibach H.I. (Ed), Bioengineering of the Skin,
274 2nd Ed, CRC Press, ISBN 0-8493-1443-7, 2004.
- 275 5. Leveque, J.L. and Querleux, B. SkinChip, a new tool for investigating the skin
276 surface in vivo. Skin Research and Technology 9, 343-347, (2003).
- 277 6. Batisse, D., Giron F. and Leveque J.L. Capacitance imaging of the skin surface.
278 Skin Research and Technology 12, pp99-104, (2006).
- 279 7. Bevilacqua, A., Gherardi, A., Guerrieri, R., "In Vivo Quantitative Evaluation of
280 Skin Ageing by Capacitance Image Analysis", IEEE Workshop on Applications of
281 Computer Vision and the IEEE Workshop on Motion and Video Computing
282 (WACV-MOTION), 2005, pp. 342-347, doi:10.1109/ACVMOT.2005.61

- 283 8. Xiao P, Singh H, Zheng X, Berg EP, Imhof RE, In-vivo Skin Imaging For
284 Hydration and Micro Relief Measurements. SCV Conference, Cardiff, UK, July
285 11-13, 2007.
- 286 9. Singh H, Xiao P, Berg P and Imhof RE, Skin Capacitance Imaging for Surface
287 Profiles and Dynamic Water Concentration Measurements, ISBS Conference,
288 Seoul, Korea, May 7-10, 2008.
- 289 10. Ou X, Pan W, Xiao P, In vivo skin capacitive imaging analysis by using grey
290 level co-occurrence matrix (GLCM), International Journal of Pharmaceutics,
291 November 2013, ISSN 0378-5173,
292 <http://dx.doi.org/10.1016/j.ijpharm.2013.10.024>.
- 293 11. Xiao, P., Ou, P., Ciortea, L.I., Berg E.P., and Imhof, R.E., "In-vivo Skin Solvent
294 Penetration Measurements Using Opto-thermal Radiometry and Fingerprint
295 Sensor", International Journal of Thermophysics, 33:1787–1794, DOI
296 10.1007/s10765-012-1318-6, 2012.
- 297 12. Taylor, H., New Techniques for Occupational Skin Health Surveillance, PhD
298 Thesis, London South Bank University, 2008.
- 299 13. Berg, E.P., Pascut, F.C., Ciortea, L.I., O'Driscoll, D., Xiao, P. and Imhof, R.R.
300 AquaFlux - A New Instrument for Water Vapour Flux Density Measurement,
301 Proceedings of the 4th International Symposium on Humidity and Moisture,

302 Center for Measurement Standards, ITRI, RoC, ISBN 957-774-423-0, 288-295,
303 (2002).

304 14. Imhof RE, De Jesus MEP, Xiao P, Ciortea LI and Berg EP, "Closed-chamber
305 transepidermal water loss measurement: microclimate, calibration and
306 performance", International Journal of Cosmetic Science, 31, 97–118, 2009.